Engineering Science and Technology, an International Journal 21 (2018) 787–797

HOSTED BY

Contents lists available at ScienceDirect

Engineering Science and Technology, an International Journal

journal homepage: www.elsevier.com/locate/jestch

Full Length Article

# Effects of process parameters on the properties of brake pad developed from seashell as reinforcement material using grey relational analysis

J. Abutu [a,*], S.A. Lawal [a], M.B. Ndaliman [a], R.A. Lafia-Araga [b], O. Adedipe [a], I.A. Choudhury [c]

[a] Department of Mechanical Engineering, School of Engineering and Engineering Technology, Federal University of Technology, Minna, Nigeria
[b] Department of Chemistry, School of Physical Sciences, Federal University of Technology, Minna, Nigeria
[c] Department of Mechanical Engineering, Faculty of Engineering, University of Malaya, 50603 Kuala Lumpur, Malaysia

ARTICLE INFO

*Article history:*
Received 8 January 2018
Revised 6 May 2018
Accepted 23 May 2018
Available online 5 June 2018

*Keywords:*
Brake pad
Non-hazardous
Grey relational analysis
Seashells
Mechanical and tribological properties

ABSTRACT

Over the years, asbestos was used as reinforcement material in brake pads production. However, due to its carcinogenic nature, it has lost its favor and there is need to find an alternative material. In this study, brake pads were produced from locally sourced non-hazardous raw materials using grey relational analysis. The materials used for production include seashell, epoxy resin (binder), graphite (friction modifier) and aluminum oxide (abrasive). Twenty- seven different samples were produced using seashell as reinforcement material by varying the process parameters. Rule of mixture was used for formulation and a weight percent of 52% reinforcement, 35% binder, 8% abrasive and 5% friction modifier were used for production. Grey relational analysis was conducted in order to scale the multi-response performance to a single response. The results indicate that optimum performance can be achieved with 14 MPa molding pressure, 160 °C molding temperature, 12 min curing time and 1 h heat treatment time. Analysis of variance shows that curing time has the least significant effect on the mechanical properties, while curing time of 24.26% and 55.23% has the most significant effect on coefficient of friction and wear rate respectively on the brake pad developed.


## 1. Introduction

Braking system is one of the basic organs which control an automobile [9]. Brake pads serve to reduce heat and wear caused as a result of the contact between mating surfaces. Frictional materials applied in automotive brake pads were formulated many years ago. Herbert Frood in the 1870s invented the earliest frictional material composed of cotton material and bitumen solution. This invention led to the establishment of Ferodo Company which still produce and supply friction materials up till date [6]. In a common brake or clutch repair work, these accumulated dusts are always wiped off before the old pads or shoes are replaced and as such, automobile mechanics are exposed to asbestos dust. Any of this method can cause particles of asbestos to become airborne. If these old brake pads are still hard enough to be applied, mechanics working on them often utilize bench grinder to normalize the surface, or dissolve the oil and dirt of the pad. Also, when replacing brake pads or shoes, the mechanic often grinds the face of the pad in order to increase the engagement process, bevel the grinding wheel edges to reduce the noise when in use, and then drill holes for riveting. These processes often lead to the release of asbestos particles which could be inhaled thereby putting the mechanic at risk of contacting diseases such as pleural, peritoneal or pericardial mesothelioma, asbestos related cancer and asbestosis [3,28]. Therefore, significant efforts have been made towards replacing fibres of asbestos in brake pads. This was reported in the work of Nakagawa et al. [26], where fibres of metals were utilized for inclusion in the production of brake pads so as to counter environmental pollution. Ibhadode and Dagwa [19], Deepika et al. [16] developed a non-asbestos-containing brake pad material using an agro-waste material base, palm kernel shell (PKS) as filler material. The authors reported that palm kernel shell was selected because it exhibited more favourable properties than the other agro-waste they investigated. Aigbodion et al. [2], Bashar et al. [6], Lawal et al. [24], Ikpambese et al. [21] and Ruzaidi et al., [29], also developed a non-asbestos brake pad by utilizing bagasse, coconut shell, palm kernel fibers and palm ash respectively as reinforcement materials. The result of their studies showed that the selected reinforcement materials were comparable with other commercially available brake pad materials. Choe-Yung et al. [14] modeled a drum brake squeal as friction excited vibration using modal assurance criterion (MAC). The study concluded that design alterations of mode

* Corresponding author.
*E-mail address:* joe4abutu@gmail.com (J. Abutu).
Peer review under responsibility of Karabuk University.

https://doi.org/10.1016/j.jestch.2018.05.014
2215-0986/

separation led to increase in system damping and the reduction of contact stiffness eliminate squeal in the friction coefficient range of $0.1 \leq \mu \leq 0.5$. Also, Ishak et al. [22] developed a one-dimensional model of leading trailing drum-type parking brake model. The results show that the torque generated by the parking brake in the downhill direction exceeds that in the uphill direction which may be due to the type of leading-trailing shoe used in the drum brake mechanism. Similarly, Khaled et al. [23] conducted series of experiments with the aim of investigating the effect of sliding speed and normal force on the coefficient of friction between brake pad and disc. The results indicated that coefficient of friction has considerable effect on disc brakes dynamics and this effect was more noticeable with wedge disc brake mechanism compared to conventional disc brake system. Belhocine and Nouby [7] developed a finite element model of the disc brake assembly with the aim of improving the understanding of the influence of Young's modulus on squeal generation. The simulation result showed that instability of the disc brake made it sensitive to Young's modulus variations of the disc brake components. Bin et al. [10] reported a modeling and control system design for the integrated electric parking brake system (IEPBs). The experiment and simulation results show that the force sensor strategy, though could reach the desired force, but could also leads to high cost and installation problems.

Grey relational analysis (GRA) is a grey system theory proposed by Deng [17] and is suitable for solving problems with complex interrelationships between multiple responses and factors, thereby reducing a research problem to a single-objective decision-making problem. [25]. Yiyo et al. [30] reported that GRA optimization procedure involves combining all performance characteristics into a particular value which can be utilized as the single characteristic in optimization problems. Therefore, in this work, seashell reinforcement materials combined with other frictional ingredients were used to develop brake pad using powder metallurgy technique. Norazlina et al. [27] reported that seashell consist primarily of calcium carbonate ($CaCO_3$), been naturally above 80% $CaCO_3$ by weight with only about 2% protein content. However, what is not known or reported in the literature is the performance of seashell as an alternative material for brake pad development, with respect to the extent to which the mechanical and tribological properties are enhanced compared to other reinforcement materials. In this paper, mechanical properties (tensile strength, compressive strength, hardness, impact strength and flexural strength) and tribological properties (coefficient of friction and wear rate) of the brake pad developed using seashell as non-hazardous reinforcement materials were evaluated. The results are discussed in a later section.

## 2. Materials and methods

### 2.1. Materials

(i) *Reinforcement materials:* the seashells shown in Fig. 1 were used as reinforcement material. Seashells (the shells of sea snails) were collected from a seafood vendor situated in Lagos bar beach, Lagos – Nigeria, while coconut shells were obtained from a coconut trader in a Sabon Tasha market in Kaduna – Nigeria.

(ii) *Binder:* Epoxy resin (Epoblock, FIP Chemicals) was used together with a co-reactant known as hardener (Sikadur 42 T, Sika Corporation U.S) to form a cross-linking reaction. These materials were obtained from a chemical store located in Onitsha, Anambra State, Nigeria.

(iii) *Friction Modifier and Abrasive Material:* Reagent grade aluminum oxide with the following specification: (Cat. No. 34143; Lot. No. 44100) was purchased from a commercial chemical shop situated in Onitsha, Anambra State, Nigeria, which served as an abrasive. Graphite powder was used as a friction modifier and was obtained from used 1.5 V TIGER head dry cell batteries.

**Fig. 1.** Seashells obtained from Bar Beach.

### 2.2. Method

The development of brake pads involved the preparation of filler materials, formulation using rule of mixture theorem, design of experiment, compression molding process, heat treatment, mechanical and tribological examination as well as optimisation using grey relational analysis (GRA).

#### 2.2.1. Materials preparation

Prior to the preparation of the seashell and graphite powder, the seashells were washed with soap and detergent, cleaned using dried cloth and were dried in a hot air oven at a temperature of 150 °C. This was followed by crushing with the seashells with pestle and mortar. They were then grinded and sieved using a sieve size of 125 μm.

#### 2.2.2. Formulation of brake pad

Samples formulation was done using rule of mixture. To use this theorem, the volume fraction and density of the individual brake pad constituents were calculated using a specified weight percent. The volume fraction for individual constituent for the seashell and coconut shell reinforced composite was calculated using Equ. 1;[4].

$$\textit{Volume Fraction of Constituent}\,(V_i) = \frac{w_i}{\rho_i} \div \sum \frac{w_j}{\rho_j} \tag{1}$$

where, $W_i$ and $W_j$ are the weight percent of the individual and total constituent respectively, $V_i$ is the volume fraction of the individual constituent. $\rho_i$ and $\rho_j$ are the densities of the individual and total constituents respectively.

The theoretical densities of the seashell and coconut shell reinforced composite can be determined by Eq. (2). [4].

$$\rho_{composite\,(seashell-based)} = \rho_s V_s + \rho_a V_a + \rho_g V_g + \rho_b V_b \tag{2}$$

where, $\rho_s$, $\rho_a$ and $\rho_b$ are the densities of the seashell, aluminum oxide, graphite and epoxy resin respectively. The density of seashell, and graphite were determined using Archimedes principle, while the densities of reagent grade aluminum oxide and epoxy resin were specified by the manufacturers.

$V_s$, $V_a$, $V_g$ and $V_b$ are the volume fraction of the seashell, aluminum oxide, graphite and epoxy resin respectively.

#### 2.2.3. Design of experiment using response surface methodology (RSM)

In this study, response surface methodology (RSM) via central composite RSM design (CCD) was used. This design method was selected in preference to Box-behnken RSM design (BBD) due to its ability to combine two-level full factorial design with additional two points (axial and centre points). It also contains the combination where all factors are at their lower and higher levels. This experimental design was built in accordance to standard RSM's

$L_{27}(2)^4$ using Minitab 17 statistical software. Table 1 shows the factor levels of process parameter where molding temperature (MT), molding pressure (MP), curing time (CT) and heat treatment time (HTT) were chosen as the process parameters that were used to analyse the tribological properties of the friction materials. Table 2 shows the experimental Matrix for RSM-Central Composite Design Layout.

*2.2.4. Production of brake pad samples*

Samples were produced using a compression molding machine (Model; 0577-86365889, Wenzhou Zhiguang Shoe-Making Machine Co. Ltd) with respect to the standard procedure specified by Chemiplastica [12] and ASTM D 4703–03. The composition of the samples were formulated using rule of mixture which remained constant throughout the molding process, while the process parameters were varied as shown in Table 2. As recommended by Chemiplastica [12], preliminary preparation involved pouring 41.06 g (23.33%) of the epoxy resin into a container, followed by the addition of 20.54 g (11.67%) of hardener (catalyst) in the ratio of 2:1. The mixture of epoxy resin and the hardener were manually stirred in a stainless steel plate until a homogenous mixture was observed. The mixture of the weighed fillers (reinforcement, abrasive and friction modifier) were also stirred manually in another stainless steel plate. The overall mixture was then transferred to a fabricated mold of size $124 \times 112 \times 10$ mm for compression molding after being stirred thoroughly in order to obtain a homogenous mixture. The final products (Fig. 2) were subjected to further heat treatment at varying time as shown in Table 2 using a hot air oven operating at a temperature of 150 °C. Belhocine [8] reported that the presence of grooves in the pads unfavorably influences the mechanical behavior of a brake pad, therefore, the heat treated samples were not grooved to ensure better performance.

**Fig. 2.** Heat treated Seashell Reinforced Brake pad Samples.

*2.2.5. Sample characterization*

The properties that were investigated during this study include tensile strength, compressive strength, hardness, impact strength,

**Table 1**
Factor levels for process parameters.

| | | Cubic Points | | Center Point | Axial Points | |
|---|---|---|---|---|---|---|
| Factors | Unit | Lower Level (−1) | Upper Level (+1) | 0 | Lower Level (−2) | Upper level (+2) |
| Moulding pressure (MP) | MPa | 12 | 16 | 14 | 10 | 18 |
| Moulding temperature (MT) | °C | 120 | 160 | 140 | 100 | 180 |
| Curing time (CT) | minutes | 6.0 | 10.0 | 8 | 4 | 12 |
| Heat treatment time (HTT) | hour | 2.0 | 4.0 | 3 | 1 | 5 |

**Table 2**
Experimental matrix for RSM-central composite design layout.

| Run | MP (MPa) | MT (°C) | CT (minute) | HTT (hour) |
|---|---|---|---|---|
| 1 | 12 | 120 | 6 | 2 |
| 2 | 16 | 120 | 6 | 2 |
| 3 | 12 | 160 | 6 | 2 |
| 4 | 16 | 160 | 6 | 2 |
| 5 | 12 | 120 | 10 | 2 |
| 6 | 16 | 120 | 10 | 2 |
| 7 | 12 | 160 | 10 | 2 |
| 8 | 16 | 160 | 10 | 2 |
| 9 | 12 | 120 | 6 | 4 |
| 10 | 16 | 120 | 6 | 4 |
| 11 | 12 | 160 | 6 | 4 |
| 12 | 16 | 160 | 6 | 4 |
| 13 | 12 | 120 | 10 | 4 |
| 14 | 16 | 120 | 10 | 4 |
| 15 | 12 | 160 | 10 | 4 |
| 16 | 16 | 160 | 10 | 4 |
| 17 | 10 | 140 | 8 | 3 |
| 18 | 18 | 140 | 8 | 3 |
| 19 | 14 | 100 | 8 | 3 |
| 20 | 14 | 180 | 8 | 3 |
| 21 | 14 | 140 | 4 | 3 |
| 22 | 14 | 140 | 12 | 3 |
| 23 | 14 | 140 | 8 | 1 |
| 24 | 14 | 140 | 8 | 5 |
| 25 | 14 | 140 | 8 | 3 |
| 26 | 14 | 140 | 8 | 3 |
| 27 | 14 | 140 | 8 | 3 |

flexural strength, coefficient of friction and wear rate. The testing procedures are discussed as follows:

*2.2.5.1. Ultimate tensile strength.* Tensile test was carried out using a Tensometer (MONSANTO; Serial No-05232) with a load beam of 600 N. This test was conducted in accordance with ASTM D638 type IV standard which specified a specimen gauge length and width of 33 and 6 mm respectively. Six specimens from each sample were prepared and labelled in compliance with ASTM D638 in type IV mode. The specimen dimensions were measured using a vernier calliper of 0.02 cm accuracy and the tests were performed by clamping each specimen between two metal fixtures (quick grips). The tensometer was then used by turning the handle located close to the ratchet wheel clockwise until failure occurred. The results obtained were used to calculate the ultimate tensile strength (UTS). The percentage elongation, UTS, and young modulus were calculated using the Eqs. (46).

$$Percentage\,(\%)\,Elongation = \frac{Elongation\,at\,break\,(E)}{Initial\,Guage\,Length\,(l_o)} \times 100 \tag{4}$$

$$Utimate\,Tensile\,Strength\,(UTS) = \frac{Maximum\,Force}{Cross\,Sectional\,Area} \tag{5}$$

$$Young\,Modulus\,(\gamma) = \frac{Tensile\,Stress\,(\sigma)}{Tensile\,Strain\,(\varepsilon)} \tag{6}$$

*2.2.5.2. Compressive strength.* Tests for compressive strength were conducted in accordance with ASTM D695 using a 100 kN Capacity universal testing machine with specifications: ENERPAC P391: Cat. Nr. 261, Norwood Instruments Ltd., Great Britain. The test specimens were placed between the surfaces of the compression tool and it was ensured that the centre line of each specimen was aligned with the plunger centre line. It was also ensured that the ends of the cubic shaped specimen dimensioned as $10 \times 10 \times 4$ mm were parallel to the surface of the compression tool. The crosshead of the testing machine was adjusted until it touched the top of the compression tool plunger. Each test specimen was then subjected to a compressive force and was gradually loaded until failure. Three specimens were tested per sample and the loads at which failure occurred as well as the deflections shown on the output display unit of the machine were recorded. An average value of the results was calculated for each test sample. The total surface area and compressive strength of the specimen were calculated using Eqs. (7) and (8) respectively.

$$\text{Total surface area(A)} = 2(bh + bt + ht) \tag{7}$$

$$Compressive\,Strength\,(CS) = \frac{Maximum\,Load\,at\,break\,(P)}{Total\,Surface\,Area\,(A)} \tag{8}$$

where b, h and t are the width, height and thickness of specimen respectively.

*2.2.5.3. Hardness.* Hardness test was conducted using a Durometer hardness tester (FRANCISCO, Munoz Irles C. B; S/N: 01554, Model: 5019, Shore D Scale). This test was performed using a loading force of 44.73 N and was carried out in accordance with the specifications in ASTM D2240 type D scale standard. The specimens were prepared to a thickness of 10 mm and were tested at three different points. The hardness was determined by the penetration depth of the indenter under the load. The hardness values of the three test points from different lining samples were recorded and the average results were calculated.

*2.2.5.4. Flexural strength.* The flexural test was conducted to measure the amount of force required to bend the brake pad samples under a three-point loading conditions. This test was conducted using a universal testing machine and specimens were tested in accordance with EN ISO 178:2003 standard which specified a specimen size of $80 \times 15 \times 10$ mm. Five specimens from each composite sample were tested and an average of three specimens with reproducible results were calculated. The test was conducted by setting the two adjustable flexural fixtures attached near the testing machine to a span of 60 mm as recommended by ISO 178:2003. This span served as the actual measured gauge length for the experiment. The loading nose and supports were aligned so that the axes of the surfaces are parallel and at midway between the two supports. The specimen was placed on the two supporting pins at set distance apart and the load (100 kN) was applied to the specimen at a specified crosshead speed of 0.6 mm/min until failure occurred. The breaking load and deflection readings were recorded, while the flexural strain, stress and modulus were calculated using Eqs. (911).

$$Bending\,(flexural)\,Stress,\ (\sigma_f) = \frac{3Pl}{2bt^2} \tag{9}$$

$$Flexural\,Strain,\ (\xi_f) = \frac{6\delta t}{l^2} \tag{10}$$

$$Flexural\,Modulus\,(Bending\,Stress),\ (\gamma_f) = \frac{Pl^3}{4b\delta t^3} = \frac{Flexural\,Stress\,(\sigma)}{Flexural\,Strain\,(\xi)} \tag{11}$$

where; $P$ = load applied to fracture the test specimen (kN), $l$ = support span (mm) and $b$ = width of test specimen (mm) and $t$ = thickness of test specimen (mm) and $\delta$ = deflection (mm).

*2.2.5.5. Impact strength test.* This test was carried out using an impact testing machine (Norwood instrument, model No: 412-07-0715269C) in charpy mode with specimens prepared in accordance to machine specification which stipulate a specimen size of $55 \times 10 \times 10$ mm with notch angle 45°, 2 mm depth and 0.25 mm radius along the base. The test was conducted according to the ASTM E23 testing procedure. The V-notched specimen was placed across the parallel jaws of the testing machine after which the pointer was set to an initial energy of 0 J. The pendulum hammer of velocity 2.887 m/s was released downward from an initial height of 425 mm towards the specimen. The absorbed energy which produced the fractured surfaces was then recorded. Three specimens were tested from each sample and the average values of the absorbed energy were recorded. The impact strength was calculated using Eq. (12) [11].

$$impact\,Strength\,(S_i) = \frac{Absorbed\,Energy\,(E)}{Thicknes\,of\,Specimen\,(f)}\ (J/mm) \tag{12}$$

*2.2.5.6. Coefficient of friction.* The test procedure used to determine the coefficient of friction of each brake pad samples was in accordance with standard organisation of Nigeria (S.O.N) recommended test practice. This procedure involved cleaning the surface of the test specimens with a dry cloth in order to get rid of any dirt that may attach to the body of the specimen. The specimen was then attached to the base of a mild steel plate (slider) with the aid of an adhesive (SUPER glue). The weight of the test specimen attached to the steel plate was measured using a digital weighing balance. Afterward, the inclined angle ($\theta$) was tilted and fixed at 15° as illustrated in Fig. 3. A cord was attached to the hook on the steel plate to connect a weight hanger of 5 N. The load of the weight hanger was gradually increased until the specimen began to slide down the surface of the plane. The value of the applied load at 0 N and the applied load when the weight of the specimen was increased were recorded. Similar procedure was followed to determine the coefficient of friction of all the produced samples. The weight (W) of the specimen attached to the steel plate and their

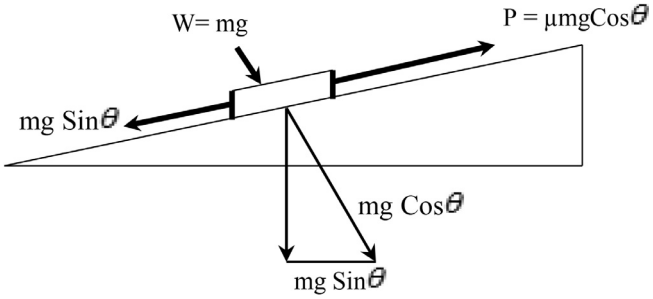


**Fig. 3.** Analysis of coefficient of static friction.

respective coefficient of friction were calculated using Eqs. ((13) and (14)). The coefficient of static friction of each sample was determined by calculating the average of the coefficient of friction using the frictional force, P.

$$W = \text{mass}(m) \times \text{acceleration due to gravity}(g) = mg \tag{13}$$

$$\text{Coefficient of friction}(\theta) = \frac{P - WSin\theta}{WCos\theta} \tag{14}$$

where, θ = angle of inclination in degree; W = Weight of mild steel plate and test specimen and P = Applied load (Frictional force).

*2.2.5.7. Wear rate.* This test was conducted in accordance with ASTM D4966-98 test standard using a Martindale abrasion testing machine (SATRA TECHNOLOGY, S/N: 11884, STM: 105, Supply-230–1-50) operating at a speed of 50 rev/min. A stainless steel disc of 135 mm diameter attached to an abrasion testing machine was coated with a detachable fabric material mounted flat on each disc of the machine to serve as the abradant. The testing procedure involved assembling the specimen holder by placing the prepared specimen of 38 mm diameter face down into the specimen holder. The assembled holder was then screwed to the testing machine according to the manufacturer's instruction after which the counter system was pre-set to record a cycle of 1000 in 1200 s. A pressure of 1.2603 MPa was applied at constant speed (50 rev/min) by a rotating wheel acting against the disc surface in the direction of abrasive flow in order to abrade the specimen surface. At the end of the pre-set cycles, the abraded particles on the surface of the abradant and the test specimen were removed. Eqs. (15) and (16) were utilized to calculate the wear rate and sliding distance.

$$Wear\,Rate = \frac{Weight\ Loss\,(L)}{Sliding\ Dis\tan ce\,(S)} \tag{15}$$

$$\text{Sliding distance}(S) = 2\pi \times N \times D \times t \tag{16}$$

where, N, D and t = radial speed, discs diameter, and time of exposure of specimen to abrasion.

## 3. Results and discussion

### 3.1. Formulation of samples using rule of mixture

The theoretical densities obtained from rule of mixture theorem shows that seashell -reinforced composite has a theoretical density of 1.159 g/cm$^3$ respectively. This predicted value is in good agreement with recommended values of commercial brake pad whose densities fall between 1.01 and 2.06 g/cm$^3$ as reported by Efendy et al. [18] and Ikpambese et al. [21].

### 3.2. Experimental results

Table 3 presents the results of the mechanical and tribological examinations performed on the brake pad samples as well as their individual signal to noise ratio values. Smaller-the better and larger-the better quality characteristics shown in Equ. 17 and 18 respectively were used to calculate the signal-to noise ratios of hardness, coefficient of friction, wear rate, tensile, impact, flexural and compressive strength of the friction materials.

$$\text{Smaller} - \text{the better}: S/N = -10\log\frac{1}{n}\left(\sum_{i=1}^{n} y_i^2\right) \tag{17}$$

$$\text{Larger} - \text{the better}: S/N = -10\log\frac{1}{n}\left(\sum_{i=1}^{n}\frac{1}{y^2}\right) \tag{18}$$

y = given factor level combination responses, n = number of factor level combination.

From the experimental results presented in Table 3, it can be observed that the UTS, compressive strength, hardness, flexural and impact strength of the brake pads vary from 1.014 to 3.63 MPa, 1.98–3.88 MPa, 52–62.67 shore D scale, 4.11–17.22 MPa and 0.056–0.133 J/mm respectively while the friction coefficient and wear rate varies from 0.43 to 0.61 and 0.105–2.613 mg/m respectively. This implies that the developed brake pads possess good mechanical and tribological properties as the results are in close agreement with the work of Dagwa and Ibhadode [15], Ademoh and Adeyemi [1] and Bala et al. [5] who reported ultimate tensile strength and hardness of 7 MPa and 72.67 (shore D scale) respectively for commercial-based brake pads. Also, The values of coefficient of friction falls within the class F (0.35–0.45), G (0.45–0.55) and H (>0.55) type of brake pads recommended for use in automobile by the Society of Automobile Engineers (SAE) while the results of wear rate are comparable with the work of Idris et al. [20] who reported a wear rate 3.80 mg/m for commercial-based brake pad.

### 3.3. Grey relational analysis (GRA)

Grey relational analysis was conducted using the procedure outlined in the work of Yiyo et al. [30]. This procedure includes using the values obtained from S/N ratio analysis shown in Table 3 to calculate the grey relational generating with larger and smaller-the better attributes given in equ. 19 and 20 respectively. This procedure was followed by scaling all performance values to 0, 1 (reference sequence definition) after which the grey relational coefficient and grades were calculated using Eqs. (21) and (22) respectively. The final process of GRA was the determination of optimal factors for the single response.

$$L\arg er - the\,better\,attributes\,(x_{ij}) = \frac{y_{ij} - \underline{y_i}}{\overline{y_i} - y_j} \tag{19}$$

$$Smaller - the\,better\,attributes\,(x_{ij}) = \frac{\overline{y}_{ij} - y_{ij}}{\overline{y_j} - \underline{y_j}} \tag{20}$$

(i = 1, 2, 3…..… m and j = 1, 2, 3…. n)where, $y_i = (y_{i1}, y_{i2}, \ldots, y_{ij}, \ldots, y_{in})$, $y_{ij}$ is the performance value of attribute j of alternative i and $\overline{y_j} = \max\{y_{ij}, i = 1, 2, \ldots, m\}$ and $\underline{y_j} = \min\{y_{ij}, i = 1, 2, \ldots, m\}$.

$$\gamma\,(x_{oj}, x_{ij}) = \frac{\Delta_{\min} + \beta\Delta_{\max}}{\Delta_{ij} + \beta\Delta_{\max}} \quad (i = 1, 2, \ldots, m \text{ and } j = 1, 2, \ldots, n) \tag{21}$$

where, $\gamma\,(x_{0j}, x_{ij})$ is the grey relational coefficient between $x_{ij}$ and $x_{0j}$,

$\Delta_{ij} = x0j - xij$, $\Delta_{\min} = \min\,(\Delta_{ij}, i = 1, 2, \ldots, m; j = 1, 2, \ldots, n)$,

$\Delta_{\max} = \max\,(\Delta_{ij}, i = 1, 2, \ldots, m; j = 1, 2, \ldots, n)$ and $\beta$ is the distinguishing coefficient, $\beta \in [0, 1]$.

The aim of the distinguishing coefficient ($\beta$) is to compress or expand the range of the grey relational coefficient and 0.5 is the widely accepted value [13]. Yiyo et al. [30] reported that after grey relational generating, $\Delta_{\max}$ will be equal to 1 and $\Delta_{\min}$ will be equal to 0.

**Table 3**
Experimental results and S/N ratio values.

| Run | Ultimate Tensile Strength (UTS) | | Compressive strength ($C_S$) | | Hardness (H) | | Flexural strength ($F_S$) | | Impact strength ($I_S$) | | Coefficient of friction (μ) | | Wear rate ($W_r$) | |
|---|---|---|---|---|---|---|---|---|---|---|---|---|---|---|
| | UTS (MPa) | S/N (η) Ratio (dB) | Compressive strength (MPa) | S/N (η) Ratio (dB) | Hardness (shore D) | S/N (η) ratio (dB) | Flexural strength (MPa) | S/N (η) ratio (dB) | Impact strength (J/mm) | S/N (η) Ratio (dB) | μ | S/N (η) Ratio (dB) | Wear rate (mg/m) | S/N (η) ratio (dB) |
| 1 | 1.43 | 18.21 | 1.98 | 5.940 | 55.00 | 34.81 | 8.130 | 18.21 | 0.07 | −23.21 | 0.49 | −6.16 | 0.33 | 9.530 |
| 2 | 2.10 | 17.25 | 2.41 | 7.630 | 57.00 | 35.12 | 7.290 | 17.25 | 0.07 | −22.81 | 0.45 | −6.99 | 0.27 | 11.42 |
| 3 | 2.65 | 20.74 | 3.12 | 9.880 | 56.33 | 35.01 | 10.89 | 20.74 | 0.08 | −21.61 | 0.55 | −5.22 | 0.24 | 12.55 |
| 4 | 2.31 | 20.02 | 2.33 | 7.340 | 54.00 | 34.65 | 10.02 | 20.02 | 0.07 | −23.26 | 0.53 | −5.53 | 0.18 | 14.73 |
| 5 | 2.16 | 15.20 | 2.30 | 7.220 | 56.00 | 34.96 | 5.750 | 15.20 | 0.06 | −24.32 | 0.56 | −5.10 | 0.40 | 7.970 |
| 6 | 2.60 | 18.40 | 2.69 | 8.590 | 53.67 | 34.59 | 8.320 | 18.40 | 0.07 | −23.01 | 0.53 | −5.60 | 0.35 | 9.030 |
| 7 | 3.02 | 21.28 | 2.69 | 8.600 | 56.33 | 35.01 | 11.59 | 21.28 | 0.12 | −18.64 | 0.58 | −4.73 | 2.61 | −8.340 |
| 8 | 1.11 | 14.24 | 2.08 | 6.350 | 54.00 | 34.65 | 5.150 | 14.24 | 0.09 | −20.88 | 0.59 | −4.54 | 0.29 | 10.81 |
| 9 | 2.27 | 16.82 | 2.67 | 8.540 | 55.33 | 34.86 | 6.940 | 16.82 | 0.10 | −20.27 | 0.57 | −4.96 | 0.24 | 12.55 |
| 10 | 3.10 | 20.95 | 2.91 | 9.290 | 55.67 | 34.91 | 11.15 | 20.95 | 0.08 | −22.32 | 0.57 | −4.85 | 0.16 | 15.72 |
| 11 | 2.14 | 21.35 | 2.87 | 9.170 | 57.00 | 35.12 | 11.68 | 21.35 | 0.09 | −20.72 | 0.57 | −4.84 | 0.26 | 11.86 |
| 12 | 3.28 | 24.55 | 2.32 | 7.320 | 54.67 | 34.76 | 16.89 | 24.55 | 0.11 | −18.88 | 0.57 | −4.91 | 0.11 | 19.07 |
| 13 | 1.34 | 21.59 | 2.70 | 8.610 | 55.33 | 34.86 | 12.01 | 21.59 | 0.08 | −22.50 | 0.43 | −7.33 | 0.21 | 13.57 |
| 14 | 1.32 | 16.09 | 1.99 | 5.960 | 54.67 | 34.76 | 6.370 | 16.09 | 0.09 | −21.29 | 0.61 | −4.29 | 0.28 | 11.01 |
| 15 | 3.16 | 24.69 | 3.88 | 11.77 | 52.00 | 34.32 | 17.17 | 24.69 | 0.11 | −18.94 | 0.53 | −5.45 | 0.19 | 14.43 |
| 16 | 3.50 | 24.67 | 2.52 | 8.040 | 62.67 | 35.94 | 17.13 | 24.67 | 0.11 | −19.40 | 0.50 | −6.09 | 0.79 | 2.020 |
| 17 | 3.28 | 23.23 | 2.82 | 9.000 | 53.67 | 34.59 | 14.50 | 23.23 | 0.09 | −20.85 | 0.57 | −4.93 | 0.18 | 14.73 |
| 18 | 1.01 | 12.27 | 2.00 | 6.010 | 52.33 | 34.38 | 4.110 | 12.27 | 0.06 | −25.08 | 0.55 | −5.26 | 0.50 | 6.060 |
| 19 | 2.84 | 23.06 | 3.47 | 10.80 | 58.00 | 35.27 | 14.23 | 23.06 | 0.09 | −20.60 | 0.52 | −5.66 | 0.12 | 18.10 |
| 20 | 1.46 | 18.33 | 2.59 | 8.250 | 54.33 | 34.70 | 8.250 | 18.33 | 0.07 | −22.51 | 0.49 | −6.18 | 0.28 | 11.01 |
| 21 | 1.97 | 20.21 | 2.80 | 8.930 | 55.00 | 34.81 | 10.24 | 20.21 | 0.06 | −23.85 | 0.57 | −4.87 | 0.22 | 13.31 |
| 22 | 2.85 | 20.90 | 2.85 | 9.100 | 56.33 | 35.01 | 11.09 | 20.90 | 0.11 | −19.57 | 0.54 | −5.29 | 2.16 | −6.670 |
| 23 | 3.90 | 24.72 | 3.51 | 10.910 | 60.33 | 35.61 | 17.22 | 24.72 | 0.13 | −17.52 | 0.51 | −5.87 | 0.11 | 19.59 |
| 24 | 2.79 | 19.56 | 2.56 | 8.160 | 59.67 | 35.52 | 9.510 | 19.56 | 0.10 | −20.26 | 0.52 | −5.70 | 0.66 | 3.680 |
| 25 | 3.63 | 22.93 | 2.63 | 8.390 | 57.33 | 35.17 | 14.01 | 22.93 | 0.09 | −20.81 | 0.50 | −6.06 | 0.22 | 13.05 |
| 26 | 3.25 | 22.83 | 2.58 | 8.240 | 58.67 | 35.37 | 13.85 | 22.83 | 0.11 | −19.53 | 0.51 | −5.83 | 0.21 | 13.57 |
| 27 | 3.41 | 23.21 | 2.76 | 8.830 | 56.00 | 34.96 | 14.48 | 23.21 | 0.11 | −19.56 | 0.50 | −6.07 | 0.20 | 13.85 |

$$\varphi(x_0, x_i) = \sum_{j=1}^{n} w_j \beta(x_{oj}, x_{ij}) \quad ; (i = 1, 2, 3 \ldots\ldots m) \tag{22}$$

*wj* represent the weight of attribute *j* which is usually dependent on the judgments of the decision maker or the structure of the proposed problem. Yiyo et al. [30] reported that $\sum_{j=1}^{n} w_j = 1$.

Table 4 shows the values of the calculated grey relational generation, grey relational coefficient (GRC) and grey relational grade (GRG) while the resulting factor effects of the process parameters are shown in Tables 5. The values in bold indicates the optimal level for each process parameters. The main effect plots obtained using the values in Table 5 are shown in Fig. 4.

**Table 4**
Grey relational generation results coefficient and grades.

| Scenario | Grey relational generation | | | | | | | Grey relational coefficient | | | | | | | Grade |
|---|---|---|---|---|---|---|---|---|---|---|---|---|---|---|---|
| | UTS | Cs | H | $F_S$ | $I_S$ | μ | $W_r$ | UTS | Cs | H | $F_S$ | $I_S$ | μ | $W_r$ | |
| $X_o$ | 1.00 | 1.00 | 1.00 | 1.00 | 1.00 | 1.00 | 1.00 | – | – | – | – | – | – | – | – |
| 1 | 0.25 | 0.00 | 0.38 | 0.48 | 0.29 | 0.39 | 0.36 | 0.4 | 0.33 | 0.45 | 0.49 | 0.41 | 0.45 | 0.44 | 0.42 |
| 2 | 0.54 | 0.29 | 0.62 | 0.40 | 0.35 | 0.11 | 0.29 | 0.52 | 0.41 | 0.57 | 0.45 | 0.44 | 0.36 | 0.41 | 0.45 |
| 3 | 0.71 | 0.68 | 0.54 | 0.68 | 0.54 | 0.69 | 0.25 | 0.63 | 0.61 | 0.52 | 0.61 | 0.52 | 0.62 | 0.40 | 0.56 |
| 4 | 0.61 | 0.24 | 0.25 | 0.62 | 0.28 | 0.59 | 0.17 | 0.56 | 0.40 | 0.40 | 0.57 | 0.41 | 0.55 | 0.38 | 0.47 |
| 5 | 0.56 | 0.22 | 0.50 | 0.23 | 0.12 | 0.73 | 0.42 | 0.53 | 0.39 | 0.50 | 0.40 | 0.36 | 0.65 | 0.46 | 0.47 |
| 6 | 0.70 | 0.45 | 0.21 | 0.49 | 0.32 | 0.57 | 0.38 | 0.62 | 0.48 | 0.39 | 0.50 | 0.42 | 0.54 | 0.45 | 0.49 |
| 7 | 0.81 | 0.46 | 0.54 | 0.72 | 1.00 | 0.86 | 1.00 | 0.73 | 0.48 | 0.52 | 0.64 | 1.00 | 0.78 | 1.00 | 0.73 |
| 8 | 0.07 | 0.07 | 0.25 | 0.16 | 0.65 | 0.92 | 0.31 | 0.35 | 0.35 | 0.40 | 0.37 | 0.59 | 0.86 | 0.42 | 0.48 |
| 9 | 0.60 | 0.45 | 0.42 | 0.37 | 0.75 | 0.78 | 0.25 | 0.55 | 0.47 | 0.46 | 0.44 | 0.66 | 0.70 | 0.40 | 0.53 |
| 10 | 0.83 | 0.57 | 0.46 | 0.70 | 0.43 | 0.82 | 0.14 | 0.74 | 0.54 | 0.48 | 0.62 | 0.47 | 0.73 | 0.37 | 0.56 |
| 11 | 0.55 | 0.55 | 0.62 | 0.73 | 0.68 | 0.82 | 0.28 | 0.53 | 0.53 | 0.57 | 0.65 | 0.61 | 0.74 | 0.41 | 0.57 |
| 12 | 0.87 | 0.24 | 0.34 | 0.99 | 0.96 | 0.8 | 0.02 | 0.79 | 0.40 | 0.43 | 0.97 | 0.93 | 0.71 | 0.34 | 0.65 |
| 13 | 0.21 | 0.46 | 0.42 | 0.75 | 0.40 | 0.00 | 0.22 | 0.39 | 0.48 | 0.46 | 0.67 | 0.45 | 0.33 | 0.39 | 0.45 |
| 14 | 0.20 | 0.00 | 0.34 | 0.31 | 0.59 | 1.00 | 0.31 | 0.38 | 0.33 | 0.43 | 0.42 | 0.55 | 1.00 | 0.42 | 0.50 |
| 15 | 0.84 | 1.00 | 0.00 | 1.00 | 0.95 | 0.62 | 0.18 | 0.76 | 1.00 | 0.33 | 1.00 | 0.91 | 0.57 | 0.38 | 0.71 |
| 16 | 0.92 | 0.36 | 1.26 | 1.00 | 0.88 | 0.41 | 0.63 | 0.86 | 0.44 | 2.05 | 0.99 | 0.81 | 0.46 | 0.57 | 0.88 |
| 17 | 0.87 | 0.52 | 0.21 | 0.88 | 0.66 | 0.79 | 0.17 | 0.79 | 0.51 | 0.39 | 0.81 | 0.59 | 0.71 | 0.38 | 0.60 |
| 18 | 0.00 | 0.01 | 0.04 | 0.00 | 0.00 | 0.68 | 0.48 | 0.33 | 0.34 | 0.34 | 0.33 | 0.33 | 0.61 | 0.49 | 0.40 |
| 19 | 0.76 | 0.83 | 0.73 | 0.87 | 0.70 | 0.55 | 0.05 | 0.68 | 0.75 | 0.65 | 0.79 | 0.62 | 0.53 | 0.35 | 0.62 |
| 20 | 0.27 | 0.40 | 0.29 | 0.49 | 0.40 | 0.38 | 0.31 | 0.41 | 0.45 | 0.41 | 0.49 | 0.45 | 0.45 | 0.42 | 0.44 |
| 21 | 0.49 | 0.51 | 0.38 | 0.64 | 0.19 | 0.81 | 0.23 | 0.50 | 0.51 | 0.45 | 0.58 | 0.38 | 0.73 | 0.39 | 0.50 |
| 22 | 0.77 | 0.54 | 0.54 | 0.69 | 0.86 | 0.67 | 0.94 | 0.68 | 0.52 | 0.52 | 0.62 | 0.78 | 0.60 | 0.89 | 0.66 |
| 23 | 1.00 | 0.85 | 1.00 | 1.00 | 1.17 | 0.48 | 0.00 | 1.00 | 0.77 | 1.00 | 1.00 | 1.53 | 0.49 | 0.33 | 0.87 |
| 24 | 0.75 | 0.38 | 0.93 | 0.59 | 0.75 | 0.54 | 0.57 | 0.67 | 0.45 | 0.87 | 0.55 | 0.66 | 0.52 | 0.54 | 0.61 |
| 25 | 0.95 | 0.42 | 0.66 | 0.86 | 0.66 | 0.42 | 0.23 | 0.90 | 0.46 | 0.59 | 0.78 | 0.60 | 0.46 | 0.40 | 0.60 |
| 26 | 0.86 | 0.39 | 0.81 | 0.85 | 0.86 | 0.49 | 0.22 | 0.79 | 0.45 | 0.73 | 0.77 | 0.78 | 0.50 | 0.39 | 0.63 |
| 27 | 0.90 | 0.49 | 0.50 | 0.88 | 0.86 | 0.41 | 0.21 | 0.83 | 0.50 | 0.50 | 0.80 | 0.78 | 0.46 | 0.39 | 0.61 |

**Table 5**
Resulting factor effects of process parameters (Average GRG).

| Factor | Level 1 (−2) | Level 2 (−1) | Level 3 (0) | Level 4 (+1) | Level 5 (+2) |
|---|---|---|---|---|---|
| MP | 0.5967 | 0.5564 | 0.6163 | 0.5610 | 0.3976 |
| MT | 0.6236 | 0.4852 | 0.6085 | 0.6321 | 0.4411 |
| CT | 0.5040 | 0.5277 | 0.5975 | 0.5897 | 0.6596 |
| HTT | 0.8748 | 0.5088 | 0.5621 | 0.6085 | 0.6077 |

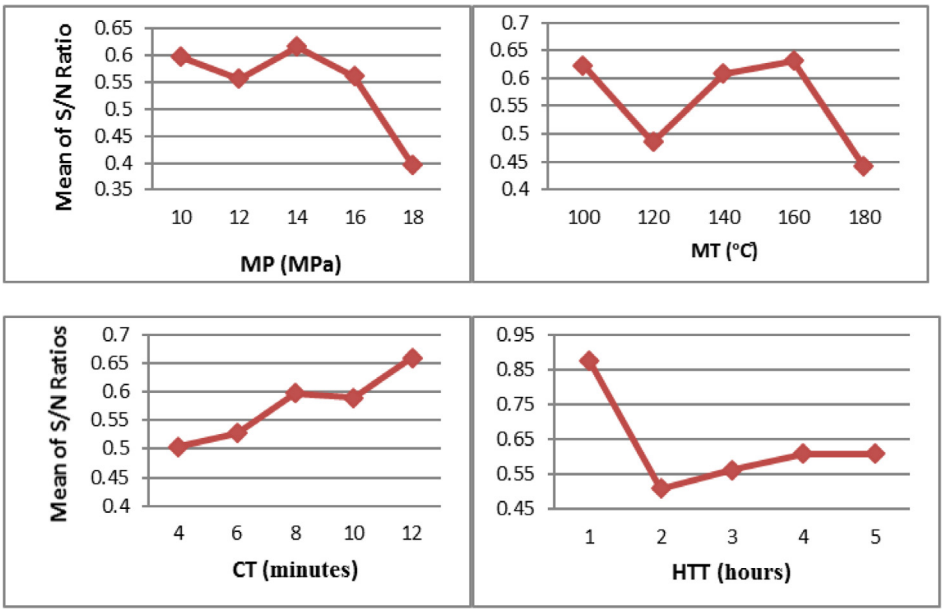


**Fig. 4.** Plots of factor effects.

From Fig. 4, it can be observed that the optimum performing seashell reinforced brake pad can be obtained using the optimal process parameters of 14 MPa moulding pressure, 160 °C moulding temperature, 12 min curing time and 1 h heat treatment time.

### 3.4. Analysis of variance (ANOVA)

Analysis of variance was conducted in order to identify the significant effects of the process parameters which affect the quality characteristics of the formulated friction materials. This analysis was conducted using $\alpha = 0.01$ significance level, at 99% confidence level. The sum of square total (SS) was calculated using equ. 23 while the values of the degree of freedom (DOF), mean square (MS), percentage contribution (P) and f values are also shown in Tables 6–12.

$$\text{Sum of Square}(SS_{\text{Total}}) = \sum_{i=1}^{n} y_{i^2} - \frac{1}{n}(y_i)^2 (\text{i} = 1, 2, 3 \ldots\ldots, 27) \quad (23)$$

where, N = number of observation (N = 27) and y = observations in *i*th sample

The ANOVA for the ultimate tensile, compressive and hardness shown in Tables 6 - 8, indicates that the moulding pressure (MP) has the highest significant effects with percentage contribution (p-value) of 42.64, 32.23 and 37.18% respectively. Also, the ANOVA for flexural strength and impact strength shown in Tables 9 and 10 indicate that the heat treatment time (HTT) has the highest significant effect with p-value of 33.87 and 33.07% respectively. The values of the tribological properties (coefficient of friction and wear rate) as shown in Tables 11 and 12 are most affected by the curing time (CT) as it shows percentage contribution of 24.26 and 55.23% respectively. The effects of all the factors on the properties of the friction materials are significant since their p-values are >0.010 (1%).

### 3.5. Regression analysis

The regression models for each output variables were obtained using MINITAB 17 software. This empirical modelling technique can be used to predict the properties of the brake pads. The optimal values (MP of 14 MPa, MT of 160 °C, CT of 12 and HTT of 1 h) obtained from grey relational analysis as shown in Fig. 4 was used to obtained the optimum performance of the seashell reinforced friction material.

**Table 6**
ANOVA for UTS.

| Factor | DOF | SS | MS | F | P (%) |
|---|---|---|---|---|---|
| MP | 4 | 7.729 | 1.932 | 20.712 | 42.64 |
| MT | 4 | 4.496 | 1.124 | 12.048 | 24.80 |
| CT | 4 | 1.908 | 0.477 | 5.1130 | 10.53 |
| HTT | 4 | 3.061 | 0.765 | 8.2028 | 16.89 |
| Error | 10 | 0.933 | 0.093 | | 5.147 |
| Total | 26 | 18.13 | 0.697 | | 100 |

**Table 7**
ANOVA for compressive strength.

| Factor | DOF | SS | MS | F | P (%) |
|---|---|---|---|---|---|
| MP | 4 | 1.749 | 0.437 | 14.01 | 32.23 |
| MT | 4 | 1.362 | 0.341 | 10.91 | 25.1 |
| CT | 4 | 0.538 | 0.134 | 4.306 | 9.912 |
| HTT | 4 | 1.465 | 0.366 | 11.73 | 27.00 |
| Error | 10 | 0.312 | 0.031 | | 5.754 |
| Total | 26 | 5.426 | 0.209 | | 100 |

**Table 8**
ANOVA for hardness.

| Factor | DOF | SS | MS | F | P (%) |
|---|---|---|---|---|---|
| MP | 4 | 55.61 | 13.901 | 22.54 | 37.18 |
| MT | 4 | 20.4 | 5.1 | 8.27 | 13.64 |
| CT | 4 | 12.08 | 3.0206 | 4.898 | 8.078 |
| HTT | 4 | 55.32 | 13.83 | 22.43 | 36.98 |
| Error | 10 | 6.167 | 0.6167 | | 4.123 |
| Total | 26 | 149.6 | 5.7529 | | 100 |

**Table 9**
ANOVA for flexural strength.

| Factor | DOF | SS | MS | F | P (%) |
|---|---|---|---|---|---|
| MP | 4 | 100.04 | 25.01 | 27.051 | 25.62 |
| MT | 4 | 125.81 | 31.45 | 34.02 | 32.22 |
| CT | 4 | 23.069 | 5.767 | 6.238 | 5.909 |
| HTT | 4 | 132.25 | 33.06 | 35.761 | 33.87 |
| Error | 10 | 9.2454 | 0.925 | | 2.368 |
| Total | 26 | 390.41 | 15.02 | | 100 |

**Table 10**
ANOVA for impact strength.

| Factor | DOF | SS | MS | F | P (%) |
|---|---|---|---|---|---|
| MP | 4 | 0.00182 | 0.000455 | 6.528 | 18.72 |
| MT | 4 | 0.002583 | 0.000646 | 9.265 | 26.57 |
| CT | 4 | 0.001407 | 0.000352 | 5.047 | 14.47 |
| HTT | 4 | 0.003215 | 0.000804 | 11.53 | 33.07 |
| Error | 10 | 0.000697 | 0.0000697 | | 7.169 |
| Total | 26 | 0.009722 | 0.000374 | | 100 |

**Table 11**
ANOVA for coefficient of friction.

| Factor | DOF | SS | MS | F | P (%) |
|---|---|---|---|---|---|
| MP | 4 | 0.0114 | 0.0029 | 11.116 | 24.02 |
| MT | 4 | 0.014 | 0.0035 | 13.605 | 29.4 |
| CT | 4 | 0.0115 | 0.0029 | 11.229 | 24.26 |
| HTT | 4 | 0.0081 | 0.002 | 7.8278 | 16.92 |
| Error | 10 | 0.0026 | 0.0003 | | 5.402 |
| Total | 26 | 0.0476 | 0.00183 | | 100 |

**Table 12**
ANOVA for wear rate.

| Factor | DOF | SS | MS | F | P (%) |
|---|---|---|---|---|---|
| MP | 4 | 1.332 | 0.3331 | 15.61 | 14.93 |
| MT | 4 | 1.518 | 0.3796 | 17.79 | 17.01 |
| CT | 4 | 4.93 | 1.2325 | 57.76 | 55.23 |
| HTT | 4 | 0.932 | 0.233 | 10.92 | 10.44 |
| Error | 10 | 0.213 | 0.0213 | | 2.391 |
| Total | 26 | 8.926 | 0.3433 | | 100 |

### 3.5.1. Ultimate tensile strength

$$\mathrm{UTS(MPa)} = 2.70 - 0.0702\mathrm{MP} + 0.00436\mathrm{MT} + 0.0153\mathrm{CT} + 0.021\mathrm{HTT} \quad (24)$$

R-sq = 63.80% and R-sq (adj) = 57.00%
Optimal value = 2.70 − 0.0702(14) + 0.00436(1 6 0) + 0.0153 (12) + 0.021(1) = 2.62 MPa

### 3.5.2. Compressive strength

$$\mathrm{CS(MPa)} = 3.79 - 0.0959\mathrm{MP} + 0.00085\mathrm{MT} + 0.0069\mathrm{CT} + 0.0157\mathrm{HTT} \quad (25)$$

R-sq = 66.60% and R-sq (adj) = 51.43%
Optimal value = 2.682 MPa

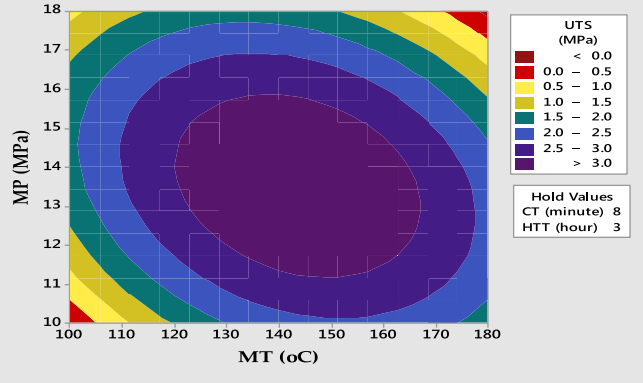


**Fig. 5.** Contour plots for UTS.

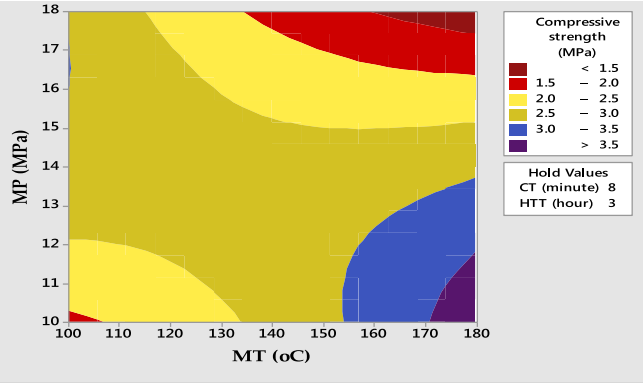


**Fig. 6.** Contour plots for compressive strength.

### 3.5.3. Hardness

$$\mathrm{Hardness} = 55.90 + 0.007\mathrm{MP} - 0.0063\mathrm{MT} + 0.049\mathrm{CT} + 0.154\mathrm{HTT} \quad (26)$$

R-sq = 79.30% and R-sq (adj) = 68.00%
Optimal value = 55.73 Shore D scale

### 3.5.4. Flexural strength (FS)

$$\mathrm{FS(MPa)} = 8.58 - 0.471\mathrm{MP} + 0.0471\mathrm{MT} + 0.046\mathrm{CT} + 0.698\mathrm{HTT} \quad (27)$$

R-sq = 57.61% and R-sq (adj) = 48.09%
Optimal value = 10.772 MPa

### 3.5.5. Impact Strength (IS) Test

$$\mathrm{IS(J/mm)} = 0.0462 - 0.00190\mathrm{MP} + 0.000293\mathrm{MT} + 0.00270\mathrm{CT} + 0.00235\mathrm{HTT} \quad (28)$$

R-sq = 60.56% and R-sq (adj) = 56.12%
Optimal value = 0.1012 J/mm

### 3.5.6. Coefficient of friction

$$\mu = 0.471 + 0.00042\mathrm{MP} + 0.000342\mathrm{MT} - 0.00050\mathrm{CT} + 0.00408\mathrm{HTT} \quad (29)$$

R-sq = 53.28% and R-sq (adj) = 50.11%
Optimal value = 0.476

### 3.5.7. Wear Rate (Wr)

$$\mathrm{Wr} = -1.79 - 0.0292\mathrm{MP} + 0.00570\mathrm{MT} + 0.1503\mathrm{CT} - 0.056\mathrm{HTT} \quad (30)$$

R-sq = 76.47% and R-sq (adj) = 63.10%
Optimal value = 0.46 mg/m.

### 3.6. Contour Plots

The contour plots for the properties of the seashell reinforced brake pads are shown in Figs. 5–11.

The contour plots shown in Figs. 5–11 indicate how change in MP (MPa) and MT (°C) affect the properties of the seashell reinforced brake pad samples while keeping the CT and HTT at 8 min and 3 h respectively. The contour levels shown in Figs. 5 and 7

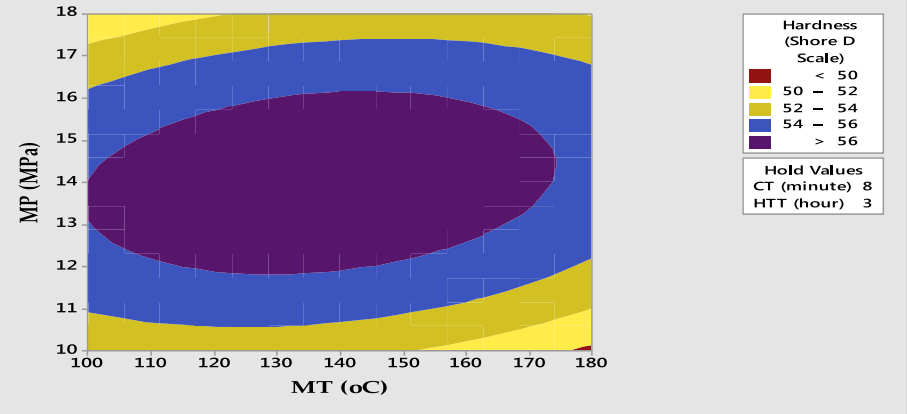


**Fig. 7.** Contour plots for hardness.

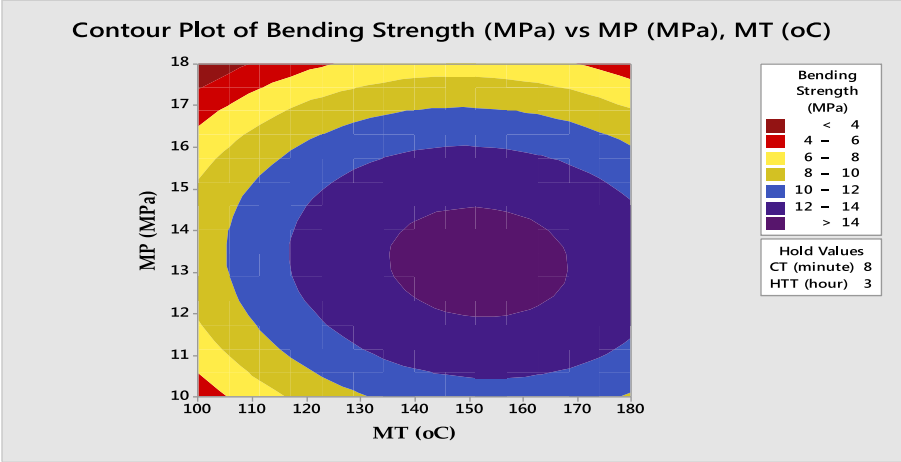


**Fig. 8.** Contour plots for flexural strength.

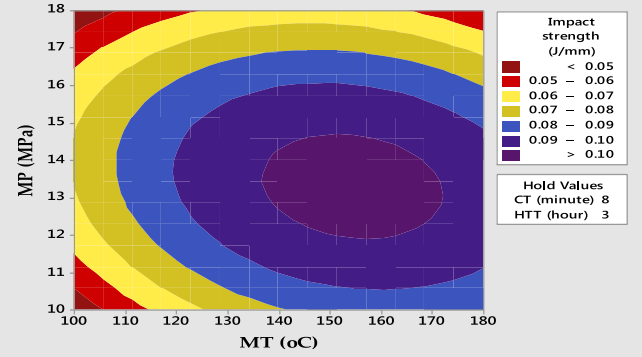


**Fig. 9.** Contour plots for Impact strength.

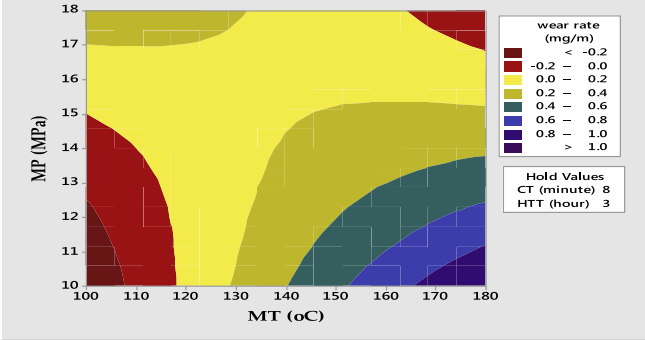


**Fig. 11.** Contour plots for wear rate.

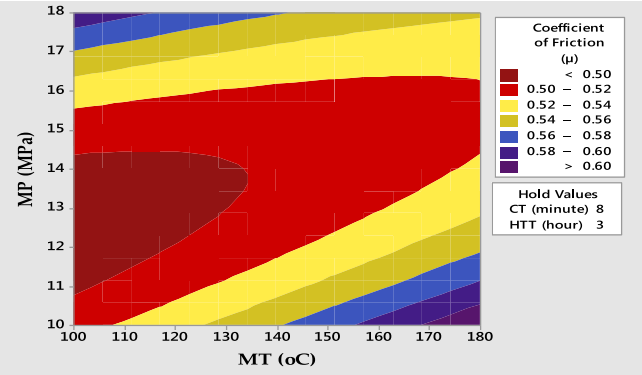


**Fig. 10.** Contour plots for coefficient of friction.

revealed that UTS of >3 MPa and hardness of >56 can be achieved using MP of 14 MPa and MT of 140 °C. Also, the contour levels shown in Figs. 8–10 revealed that flexural strength of >14 MPa, impact strength of >0.1 J/mm and coefficient of 0.52–0.54 can be achieved using MP of 13 MPa and MT of 150 °C while Fig. 6 shows that compressive strength of >3.5 MPa can be achieved using MP of 10.5 MPa and MT of 175 °C. Finally, from Fig. 11, it can be observed that a wear rate of 0–0.2 mg/m can be obtained using MP of 13 MPa and MT of 125 °C

## 4. Conclusions

Seashell was used as non-hazardous reinforcement material to produce brake pad composite. The newly developed material was investigated by determining its mechanical and tribological properties. The following conclusions can be drawn:

1. The performance of the newly developed brake pads compare favorably with commercially available as reported in the literature.
2. Changes in the process parameters (MP, MT, CT and HTT) affect the properties of the materials as all the developed brake pads produced with varying process parameters gave different performance values.
3. From the grey relational analysis conducted, it can be concluded that the seashell reinforced brake pad may be produced using 14 MPa molding pressure, MT of 160 °C molding temperature, 12 min curing time and 1 h heat treatment time.
4. Finally, the developed brake pads gave a better friction coefficient as the optimal value (0.48) falls within the class G (0.45–0.55) type of brake pads recommended for use in automobile by the Society of Automobile Engineers (SAE).
5. The effects of all the factors on the mechanical and tribological properties of the brake pads are significant as their p-values are >0.010 (1%).

## Acknowledgement

The authors are grateful to the management of Federal University of Technology Minna – Nigeria for the grant (Senate/FUT-MINNA/2015/03) allocated to this research.

## References

[1] A.N. Ademoh I.O. Adeyemi 2015 Development and evaluation of maize husks (asbestos-free) based brake pad Indus. Eng. Lett. – IEL 5 2 67–80.
[2] V.S. Aigbodion, J.O. Agunsoye, S.B. Hassan, F. Asuke, U. Akadike, Development of Asbestos-free Brake pad using Bagasse, Tribol. Indust. 32 (1) (2010).
[3] E. Anon Automotive Brake Repairs Trends and Safety Issues Retrieved from http//www.sirim.my/amtee/pm/brake.hltm 2004.
[4] D.R. Askeland, The Science and Engineering of Materials, Massachusetts, PWS Publishers, U.S.A, 1985.
[5] K.C. Bala, M. Okoli, M.S. Abolarin, Development of automobile brake pad using pulverized cow hooves, Leonardo J. Sci. 15 (28) (2016) 95–108.
[6] D. Bashar B.M. Peter M. Joseph 2012 Effect of material selection and production of a cold-worked composite brake pad J. Eng. Pure Appl. Sci. 2 3 24
[7] A. Belhocine, M. Nouby, Effects of Young's Modulus on disc brake squeal using finite element analysis, Int. J. Acoust. Vibrat. 21 (3) (2016) 292–300.
[8] A. Belhocine, FE prediction of thermal performance and stresses in an automotive disc brake system, Int. J. Adv. Manuf. Technol. 89 (2017) 3563–3578.
[9] A. Belhocine, W.O. Wan Zaidi, CFD analysis of the brake disc and the wheel house through air flow: predictions of Surface heat transfer coefficients (STHC) during braking operation, J. Mech. Sci. Technol. 32 (1) (2018) 481–490.
[10] W. Bin, G. Xuexun, Z. Chengcai, X. Zhe, Z. Jie, Modeling and control of an integrated electric parking brake system, J. Franklin Inst. 352 (2015) 626–644.
[11] L.N. Clara, F.P. Jane Maria, C.R. Mirabel, Effect of the interfacial adhesion on the tensile and impact properties of carbon fiber reinforced polypropylene matrices, J. Mater. Res. 8 (1) (2005) 1516–11439.
[12] Chemiplastica (2010), Thermoset Processing Manual Compression Molding, Retrieved from, http://www.chemiplastica.com/pdf/compression-molding-guidelines.pdf.
[13] P.F. Chin, Manufacturing process optimization for wear property of fiber-reinforced polybutylene terephthalate composites with grey relational analysis, Wear 254 (2003) 298–306.
[14] T. Choe-Yung, M.R. Zaidi, N.A. Muhammad, H., Analysis of friction excited vibration of drum brake squeal, Int. J. Mech. Sci. 67 (2013) 59–69.
[15] I.M. Dagwa, A.O.A. Ibhadode, Some Mechanical and Physical properties of Asbestos–free Experimental brake pad, J. Raw Mater. Res. 2006 2. Retrieved from Issue http://www.scielo.br/scielo.php?script=sci_arttext&pid=S1678587820080002000010&lng=en&nrm=iso&tlng=en
[16] K. Deepika, R.C. Bhaskar, R.D. Ramana, Fabrication and performance evaluation of a composite material for wear resistance application, Int. J. Eng. Sci. Innov. Technol. 2 (2013) 6.
[17] J. Deng, Control problems of grey systems, Syst. Control Lett. 1 (5) (1982) 288–294.
[18] Efendy, H., Wan-Mochamad, W. M., Yusuf, N. B. M., (2010). Development of natural fiber in Non-metallic brake friction material. Seminar Nasional Tahunan Teknik Mesin (SNTTM), 13–15, Ke-9 Palembang.
[19] A.O.A. Ibhadode, I.M. Dagwa, Development of asbestos-free friction pad material from palm kernel shell, J. Braz. Soc. Mech. Sci. Eng. 30 (2) (2008) 166173.
[20] U.D. Idris, I.J. Abubakar, C.I. Nwoye, V.S. Aigbodiun, Eco-friendly Asbestos free brake-pad: using banana peels, J. Eng. Sci. (2015) 1018–3639.
[21] K.K. Ikpambese, D.T. Gundu, L.T. Tuleu, Evaluation of palm kernel fibers (PKFs) for production of asbestos-free automotive brake pads, J. King Saud Univ. – Eng. Sci. 28 (1) (2014) 110–118.
[22] M.R. Ishak, A.R. Abu Bakar, A. Belhocine, J. Mohd Tayeb, W.O. Wan Zaidi, Brake torque analysis of fully mechanical parking brake system: theoretical and experimental approach, Measurement 94 (2016) 487–497.
[23] R. Khaled, M. Mahmoud, M. Mourad, M.A. Bin, Dynamic behaviors of a wedge disc brake, Appl. Acoust. 128 (2017) 32–39.
[24] Lawal, S. A., Ugwuoke, I. C., Abutu, J., Lafia-Araga, R. A., Dagwa, I. M., Kariim, I. (2016).Rubber Scrap as Reinforced Material in the Production of Environmentally Friendly Brake Pad. Reference Module in Materials Science and Materials Engineering. Oxford: Elsevier; 1-10.
[25] J. Morán, E. Granada, J. Míguez, Porteriro,, Use of grey relational analysis to assess and optimize small biomass boilers, Fuel Process. Technol. 87 (2) (2006) 123–127.
[26] T. Nakagawa, M. Ishi, K. Suzuki, M. Yanada, K. Ito, Development of Technology for producing Short-Length Metal Fiber by Chatter Machining, Research and Development in Japan, The Okochi Memorial prize, 1986, pp. 45–50.
[27] H. Norazlina, A.R.M. Fahmi, W.M. Hafizuddin, $CaCO_3$ from seashells as a reinforcing filler for natural rubber, J. Mech. Eng. Sci. 8 (2015) 1481–1488.
[28] R.L. Norton, Machine Design: An Integrated Approach, 2nd., Addison Wesley Longman, Singapore, 2001.
[29] C.M. Ruzaidi A.B. Mustafa J.B. Shamsul Alida A. Kamarudin H. (2011). Morphology and Wear Properties of Palm Ash and PCB Waste Brake Pad. International Conference on Asia Agriculture and Animal IPCBEE vol.1, IACSIT Press, Singapore.
[30] K. Yiyo, Y. Taho, W.H. Guan, The use of a grey-based Taguchi method for optimizing multi-response simulation problems, Eng. Optim. 40 (6) (2008) 517–528.